Applied Energy 213 (2018) 158–168

Contents lists available at ScienceDirect

Applied Energy

journal homepage: www.elsevier.com/locate/apenergy

Slow pyrolysis of organic fraction of municipal solid waste (OFMSW): Characterisation of products and screening of the aqueous liquid product for anaerobic digestion

Y. Yang[a,*], S. Heaven[b,*], N. Venetsaneas[b], C.J. Banks[b], A.V. Bridgwater[a]

[a] BioEnergy Research Group, European Bioenergy Research Institute, Aston University, Birmingham B4 7ET, UK
[b] Faculty of Engineering and the Environment, University of Southampton, Southampton SO17 1BJ, UK

HIGHLIGHTS

- Slow pyrolysis and anaerobic digestion were integrated for energy recovery from waste.
- Aqueous pyrolysis liquids produced from OFMSW were screened in AD trials.
- Pyrolysis temperature was key factor for liquid yield, energy content, toxicity and COD.
- Organic pyrolysis liquids contain 18.9–63.0% of the product energy.
- Aqueous product contains 1.2–13.1% of product energy and about 50% convertible to CH_4.

ARTICLE INFO

Keywords:
Municipal solid waste
Slow pyrolysis
Anaerobic digestion
Aqueous fraction of pyrolysis liquid
Toxicity assay
Statistical analysis

ABSTRACT

A comprehensive study of the energy yield from slow pyrolysis of the organic fraction of municipal solid waste (OFMSW) and energy recovery from the aqueous liquid product by anaerobic digestion has been carried out. In this paper, the results of the liquid pyrolysis product characterisation are presented, with toxicity and methane potential assessments of the aqueous liquid product. The OFMSW feedstock was obtained from a UK waste treatment plant. Shredded samples dried to different moisture contents (12.7–45.8%) were processed in a 300 g per hour auger screw pyrolysis reactor at temperatures from 450 to 850 °C. Sixteen pyrolysis runs were performed, with process mass balance closures above 90% obtained (wet feed basis). Pyrolysis liquids showed clear phase separation under gravity. With increasing processing temperature, the liquid yield (both organic and aqueous fraction) reduced but the gas yield increased. An investigation into the product energy distribution indicated that processing temperature had a strong effect on the product energy distribution, while the effect of feedstock moisture was relatively small. Batch anaerobic testing of the aqueous fraction showed that toxicity increased with pyrolysis processing temperature and decreased with feedstock moisture content. Statistical analysis confirmed that the pyrolysis processing temperature was the dominant factor affecting the toxicity of the aqueous product. Careful acclimatisation of the microbial consortium to the applied substrate and loading is likely to be necessary for improved digestion of the aqueous fraction.

1. Introduction

Over the past 20 years, the focus of waste management in EU countries has increasingly moved from disposal to prevention, reuse or recycling, or recovery. This has led to a fall in the proportion of municipal solid waste (MSW) sent to landfill from 64% in 1995 to 25% in 2015, with a corresponding increase for alternative approaches [1]. Energy recovery through waste-to-energy processes has contributed to this change and, although it has low priority in the waste management hierarchy, it can provide an effective means of organic waste treatment, sustainable energy generation and resource recovery. Across the EU, an average of 26.6% municipal waste generated in 2015 was incinerated

Abbreviations: AD, anaerobic digestion; ANOVA, analysis of variance; ASTM, American Society for Testing and Materials; cnSMP, cumulative net specific methane production; COD, chemical oxygen demand; DCL, dichlorophenol; EC50, half maximal effective concentration; FID, flame ionisation detector; GC–MS, gas chromatograph–mass spectrometer; HTC, hydrothermal carbonisation; ICP, inductively coupled plasma; KF, Karl Fischer; OFMSW, organic fraction of municipal solid waste; TGA, thermogravimetric analysis; TS, total solids; VOC, volatile organic compound; VS, volatile solids; WW, wet weight

* Corresponding authors.
E-mail addresses: y.yang6@aston.ac.uk (Y. Yang), s.heaven@soton.ac.uk (S. Heaven).

https://doi.org/10.1016/j.apenergy.2018.01.018
Received 15 November 2017; Received in revised form 3 January 2018; Accepted 5 January 2018
Available online 28 January 2018

and 16.6% was biologically treated: both processing methods increased by over 10% compared to 1995 levels [1]. In many cases, however, this total processing capacity is in the form of conventional incineration or aerobic biological treatment: while highly effective at stabilising organic matter, these systems may not maximise the energy and resource recovery potential [2,3]. Considerable research and industrial development is therefore currently focused on seeking more efficient and sustainable processing methods with higher value products to meet the anticipated growth in the EU's waste processing market and maximise the benefits of waste conversion [4].

Pyrolysis is a thermochemical conversion process that has been widely used for centuries in the manufacture of charcoal. More recently, it has been the subject of extensive research as a means of processing organic waste for energy recovery, and in particular for converting solid biomass into valuable liquid and gaseous biofuels as well as charcoal [5–7]. Pyrolysis is thermal decomposition occurring in the absence of oxygen. Organic materials are converted to form liquid, gaseous and solid products that can be used as chemicals, biochar and biofuels which may require upgrading to minimise emissions of hazardous gases (e.g. nitrogen and sulphur oxides) and particulates [5,8]. Pyrolysis processes include fast pyrolysis that employs a high heating rate, short hot vapour residence time and rapid vapour cooling to maximise liquid yield; and slow pyrolysis that employs a relatively slow heating rate and long residence time to maximise the solid product. In contrast, anaerobic digestion (AD) is a biological process that is particularly suitable for wet wastes and produces biogas (a mixture of CO2 and methane) with a semi-solid residue digestate. It has seen increasingly widespread adoption in recent years for the treatment of source segregated organic wastes due to the recovery of a valuable fuel gas and the environmental benefits associated with the process [9], including use of the digestate which may have value as a source of plant nutrients [10].

Linking pyrolysis and AD in an integrated waste treatment process is interesting, as this may offer a means of valorising unusable by-products from the upstream process in the downstream process, potentially increasing the overall energy yield [11–14] and the opportunities for energy recovery from waste. An example is recovery of energy from the aqueous fraction of the pyrolysis liquid which might otherwise be lost or even incur a disposal cost. Recently, some pioneering work has addressed this topic. Hubner and Mumme [15] studied the AD of aqueous products from slow pyrolysis of digestate in a bench-scale rotary kiln reactor. The AD experiments were carried out in mesophilic conditions (40.5 °C) in batch tests with durations of 49–69 days using an unadapted inoculum and initial values of substrate chemical oxygen demand (COD) from 3 to 30 g L^{-1}. This work claimed that most of the volatile organic compounds (VOCs) in the liquid samples, such as levoglusosan, furfural and phenol, could be converted into biogas without the addition of biochar. Initial COD concentrations up to 12 g L^{-1} were tolerated and COD removal rates of up to 63% were achieved. Liquid samples from lower pyrolysis temperatures (330–430 °C) performed better than those from higher temperatures in terms of COD degradation. Torri and Fabbri [16] investigated the AD of aqueous product from the slow pyrolysis of cornstalk at 400 °C in a fixed bed reactor. AD tests were carried out in 100 mL syringe reactors for micro-batch and semi-continuous tests. Biomethane production was observed, but the methane yield was low at 34% of the theoretical value based on COD. With addition of cornstalk char in the pyrolysis liquid, the yield of methane increased to about 60% of the theoretical value, and the biogas methane content remained stable for the 220-day test period. The authors suggested that this effect was due to the ability of porous char to reduce the toxicity of pyrolysis liquid through selective adsorption favouring the removal of more hydrophobic and toxic furans above that of the more hydrophilic and digestible sugars, which remained in the aqueous phase [17]. Apart from pyrolysis, similar work has also been conducted on linking AD and hydrothermal carbonisation (HTC), which employs water in processing with different temperature and pressure compared to pyrolysis. Erdogan et al. [18] investigated the HTC of orange pomace and performed anaerobic batch tests on the aqueous phase of the HTC product to determine the resulting biogas and methane potential. Measurement of the COD and total organic carbon (TOC) showed that the liquid samples from higher HTC processing temperature gave lower TOC and COD concentrations. Biogas yield testing (batch fermentation) was carried out in 100 mL syringes at 42 °C for 15 days. It was found that the daily biogas production increased rapidly in the first 7 days but then decreased. The cumulative methane yields marginally decreased with increasing HTC processing temperature. In a different integration mode, Monlau et al. demonstrated the feasibility of coupling pyrolysis to AD as a downstream process. The authors claimed that integrated process could improve the overall energy recovery efficiency by 42% compared to a standalone process [19,20].

Prior to the present work, no research has been found on linking pyrolysis with downstream AD of MSW or related waste materials. This work presents the results of processing the organic fraction of municipal solid waste (OFMSW) in a slow pyrolysis system under an extensive matrix of processing conditions. All liquid, gaseous and solid products were collected and their product energy distributions were analysed. The aqueous fractions of the liquid products were tested for their anaerobic toxicity and biodegradability in batch screening tests. The overall process mass balances under various processing conditions were determined and evaluated. Statistical analysis was employed to assess the effect of processing condition on the process mass balance, product energy distribution and the results of AD screening.

2. Materials and methods

2.1. Feedstock

The feedstock was obtained from Biffa Group Ltd's waste treatment plant in Leicester, UK. The original MSW was collected from households. After mechanical removal of the majority of metals, paper/cardboard, glass and plastics, the raw material mainly consists of the organic fraction of MSW (OFMSW), which comprises small pieces of biomass (wood and grass), plastics, decomposed materials (such as from food waste and paper) and inorganics including metal, ceramics, sand etc. This material was further screened and shredded to reduce its particle size to less than 10 mm for ease of use in the pyrolysis experiments. An illustration of the feedstock samples is shown in Fig. S1.

The characterisation of the as-received feedstock is shown in Table 1. It has a high moisture content (45.8 wt% as received on a wet basis) and high ash content (23.1 wt% wet basis), and the proportions of carbon and oxygen are similar at around 45% (on a dry and ash free

Table 1
Proximate and ultimate analysis of MSW feedstock.

	Unit	Value
Ultimate analysis[a]		
C	TS%	35.1
H	TS%	4.7
N	TS%	1.4
S	TS%	0.2
O[b]	TS%	16.1
Proximate analysis		
Moisture[c]	wt.%	45.8
Volatiles[a]	TS%	51.1
Fixed carbon[a]	TS%	6.3
Ash content[a]	TS%	42.6
Measured HHV[a]	MJ kg^{-1} dry mass	15.4
Theoretical HHV[a,d]	MJ kg^{-1} dry mass	15.3

[a] Presented on an oven-dried mass basis.
[b] Oxygen content was calculated by difference.
[c] Moisture content is presented on a wet mass basis.
[d] Theoretical HHV calculated according to [24].

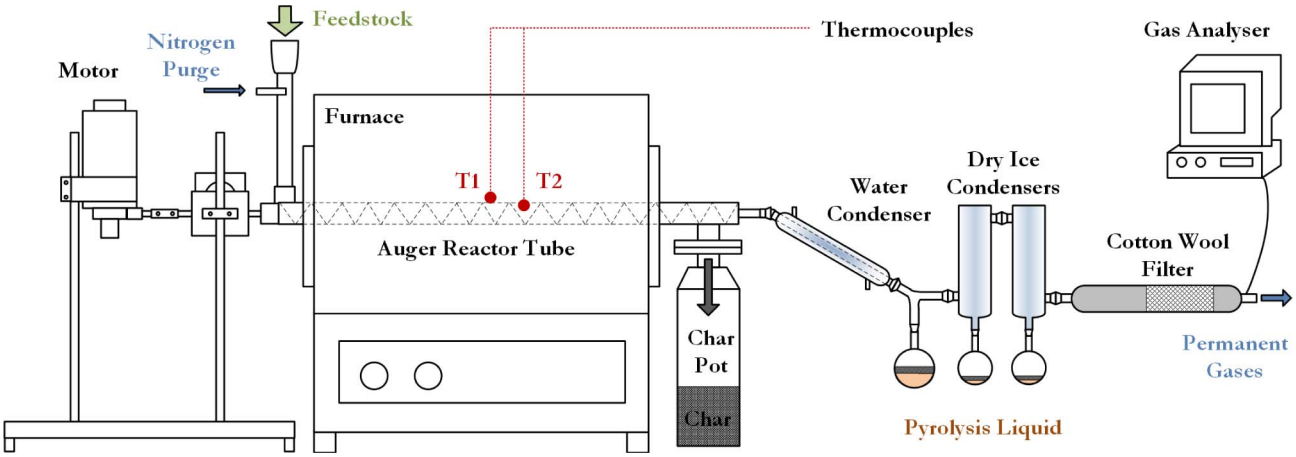

Fig. 1. Schematic diagram of the bench-scale pyrolysis system.

basis). Because of concerns over inhomogeneity, the results are a trimmed mean from the analysis of 10 samples. The results of Inductively Coupled Plasma (ICP) for comprehensive analysis of elements contained are presented in Table S1 in the Supplementary Material.

2.2. Slow pyrolysis system and process condition matrix

2.2.1. Slow pyrolysis system

The pyrolysis system consists of a bench-scale continuous auger pyrolysis reactor, a solid product collection vessel and a liquid product condensation and collection system, as shown in Fig. 1 [21]. The reactor tube has a diameter of 26.5 mm and a length of 500 mm, and is externally heated by a Carbolite VST 12/400 electric furnace with a power capacity of 2 kW. Before the start of any pyrolysis experiment, the reactor is purged with nitrogen to eliminate any oxygen present in the reactor tube.

Feedstock is fed manually through a feeding chute at a constant feeding rate of 350 g per hour. Once in the reactor, the material is transported by the auger screw along the length of the reactor tube for thermal processing. The evolved pyrolysis vapours and gases pass through a cold-water condenser (at 5 °C) and two dry ice condensers (at −70 °C), where the vapour is cooled to form pyrolysis liquid, which contains an organic fraction and an aqueous fraction. The liquid samples from three collection bottles were mixed for analysis. The permanent gases finally pass through a horizontal tube with a cotton wool filter to absorb aerosols. Before venting, a sample stream of the gas is sent to a Micro GC analyser for gas analysis.

The solids residence time is the time taken for the solid feedstock to travel through the length of the reactor tube. At the given feed rate and at an auger rotation speed of 5 rpm, the solids residence time is approximately 6 min. The vapour residence time is the time taken for the vapour product to travel the length of the reactor: under a constant feed rate and auger rotation speed the vapour residence times are calculated as being in the range of 7–17 s depending on reaction temperature. For this reactor with a certain raw material and a fixed feed rate, the vapour residence time is a function of the vapour production rate, which is dependent on the thermal processing temperature: the higher the reaction temperature, the higher the vapour production rate, and the shorter vapour residence time, which is calculated for each run. The temperatures of the furnace, the reactor outer surface, the reactor inner surface and the vapour outlet are measured respectively by using K-type thermocouples and recorded in a data logger. Mass balances (wt% on a wet weight basis) were calculated based on the mass of waste processed and the final products collected of pyrolysis liquid, char, and non-condensable gases.

2.2.2. Process conditions

The experimental design consisted of a matrix containing a total of sixteen pyrolysis experiments using OFMSW feedstock at four different initial moisture contents (45.8, 34.6, 22.8 and 12.7 wt% on wet feed basis) and four different furnace temperatures (450, 550, 700 and 850 °C at the outside wall of the reactor). There were two temperature measurement points on the outside wall (T1) and the inside wall (T2) of the reactor tube respectively, representing the pyrolysis processing temperature applied to the reactor and the reaction temperature of the pyrolysis process (shown in Fig. 1).

It is worth noting that the processing temperature applied to the reactor tube is different from the actual reaction temperature. This is because that the reactor tube is externally heated but there is a lack of effective heat transfer medium (for example a fluidising sand) between the reactor inner wall and the processed feedstock. A temperature gradient thus exists between the feedstock and reactor wall. The gradients between T1 and T2 in different runs are presented in Table S2.

Each pyrolysis run lasted at least one hour to ensure sufficient liquid product (at least 100 mL aqueous product) was produced for characterisation and AD experiments.

2.3. Product analysis and characterisation

A Thermo Flash 2000 elemental analyser was used to determine the elemental composition of all solid and liquid samples. The contents of carbon, hydrogen, nitrogen and sulphur (wt.%) of total solids on oven-dried basis were analysed in triplicate and average values were presented. The oxygen content was obtained by difference.

The ash content of solid samples was calculated in accordance with the ASTM E1755 method on a moisture free basis. Prior to the analysis, the feedstock sample was dried at 60 °C ± 2 °C for 24 h. OFMSW samples of around 15 g were placed in a Carbolite AAF1100 furnace and heated to 575 °C for 6 h. The crucibles were then removed from the furnace and cooled in a desiccator. The crucible was weighted and then replaced in the furnace at 575 °C for a further hour, cooled and re-weighed. This step was repeated until the weights were within 0.1 mg.

Thermogravimetric analysis (TGA) for solid samples was performed using a Perkin Elmer Pyris 1 thermogravimetric analyser. The pyrolysis TG characterisation programme was set as: (1) Hold for 10 min at 60 °C; (2) Heat from 60 °C to 900 °C at 20 °C min^{-1}; (3) Hold for 10 min at 900 °C; (4) Cool from 850 °C to 60 °C at 40 °C min^{-1}. All analyses were performed in triplicate and averages taken.

The higher heating values (HHV) of the solid and liquid samples were measured in accordance with the ASTM D420 method using a Parr 6100 calorimeter. In addition, the HHV was also calculated from the elemental analysis and the results of both methods were compared.

The chemical composition of the liquid samples was analysed using

a Varian 450 gas chromatograph (GC) coupled to a 220 mass spectrometer (MS) with a flame ionisation detector (FID) and an Agilent J&W VF-5 ms column (L: 30 m, ID: 0.25 mm and DF 0.25 μm). Helium was used as the carrier gas. HPLC grade acetone was used to dilute the liquid sample for analysis. The GC injection port was maintained at 275 °C and the oven was heated at 5 °C min^{-1} from 45 to 280 °C. The FID detector was held at 275 °C. Proposed assignments of peaks from the analysis chromatograph were made based on mass spectra from the NIST 2011 MS library.

The pH values of the liquids were determined using a Sartorius PB-11 pH Meter calibrated with buffers at pH 3, 7, and 13 before each measurement. All measurements were performed in triplicate and average values were reported.

The water content of the pyrolysis liquid samples was determined using a Mettler Toledo V30 Compact Volumetric Karl Fischer (KF) titrator with Hydranal (R) K as a working medium and Hydranal (R) Composite 5 K as a titrant. Runs were performed in triplicate and average values are presented.

An on-line Varian CP 4900 MicroGC coupled to a thermal conductivity detector (TCD) was used for compositional analysis of the permanent gases. Hydrogen, oxygen, carbon monoxide and methane were analysed in two gas columns (Varian CP-5A Molsieve and CP-PortaPLOT) with a sample injection interval of 150 s.

Total solids (TS) and volatile solids (VS) on wet feed basis were determined for anaerobic digestion inoculum according to Standard Method 2540 G [22]. The COD of the aqueous fraction was measured using a mercury-free large-scale (10 mL) flask digestion procedure with chromium (III) potassium sulphate and silver nitrate solutions [23].

Biogas composition (CH_4 and CO_2) was determined using a Varian star 3400 CX Gas Chromatograph fitted with a gas sampling loop, a packed stainless steel SUPELCO 80/100 mesh porapack-Q column and a TCD detector, and with argon as the carrier gas at a flow of 25 mL min^{-1}. The GC was calibrated with a standard gas of 65% CH_4 and 35% CO_2 (v/v) (BOC Ltd, UK).

2.4. AD trial for liquid product

Screening tests were carried out based on an extended form of the assay in BS ISO 13641-1:2003, in which specific methane production was also estimated by determination of gas composition at the end of the incubation period.

The inoculum was digestate from a mesophilic anaerobic digestion plant treating municipal wastewater biosolids at Millbrook Wastewater Treatment Plant, Southampton, UK. The inoculum was sieved before use and had the following typical characteristics: TS 4.1% of wet weight (WW), VS 2.8%WW, COD 41 g L^{-1}, pH 7.4. Tests were carried out in 120 mL glass serum bottles containing 40 g of inoculum and 0.5 mL of a nutrient stock solution containing 100 g L^{-1} each of nutrient broth, yeast extract and glucose. Tests were conducted at inoculum to substrate (i/s) ratios of 4:1, 8:1, 16:1 and 32:1 on a VS:COD basis. The quantity of test compound added varied depending on the required strength; the final volume was then made up to 50.5 mL with deionized water. Samples were tested in duplicate with four blank controls (inoculum plus nutrient solution only), and three positive controls containing 0.35 mL of 3,5-dichlorophenol (3,5-DCL) at 70 mg L^{-1} as a reference compound of known toxicity. After sparging the headspace with nitrogen the serum bottles were incubated at 37 °C for up to 115 h. Pressure was measured using a Digitron 2025P meter (Digitron, UK) at 0.5, 1.0, 1.5, 2.0, 2.5, 3.5 and 4.5 days from the start of the test. The EC50 value in which the biogas production is inhibited by 50% in comparison with that of the blank controls was calculated from the results after 48 h. After each pressure measurement the headspace gas was released into a foil-lined gas-impermeable sampling bag, and at the end of the run the gas composition was measured and normalised to account for the initial nitrogen content. The result was used to estimate the final specific methane production by deducting the methane production of the inoculum-only controls and dividing by the amount of COD added.

2.5. Statistical analysis

Regression analysis was employed to compare experimental values between two parameters. Analysis of variance (ANOVA) and *t*-test (two-sample assuming equal variances) were used to determine the statistical significance of paired variables, based on a critical p-value of less than 0.05.

3. Results and discussion

3.1. Feedstock analysis

Detailed sample characterisation, including proximate and ultimate analyses, for the OFMSW is given in Table 1. The carbon (C), hydrogen (H), and nitrogen (N) sulphur (S) analyses were: C 35.1%, H 4.7%, N 1.4% and S 0.2% (accuracy ± 0.3% absolute). Proximate analysis showed the sample consisted of 51.1% volatiles and 6.3% fixed carbon, with a heating value of 15.4 MJ kg^{-1} on a dry material basis. This shows an excellent agreement with the theoretical HHV calculated from the Dulong equation [24], thus supporting the accuracy of the elemental analysis results.

Fig. 2 shows the results of TG analysis for the OFMSW samples. It can be clearly seen that the decomposition of the samples started at

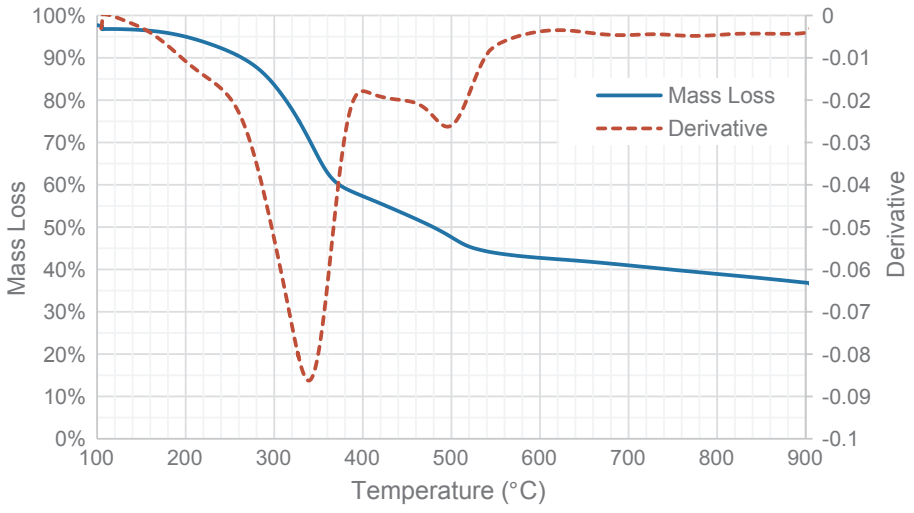

Fig. 2. Pyrolysis TGA curves of OFMSW sample.

around 120 °C. Major mass loss occurs in the temperature range of 250–550 °C, during which volatile matter is released with the formation of char and evolution of pyrolysis gases [25–27]. Two peaks are seen in the derivative of mass loss, at around 340 and 500 °C, respectively. These are likely to correspond to the major decomposition temperatures of key components of the OFMSW, i.e. paper (hemicellulose and cellulose) and mixed plastics, respectively.

3.2. Mass balances

Mass balances for the pyrolysis runs under the matrix of processing conditions are discussed in this section. Since the original OFMSW feedstock used in this work had a considerably high moisture and high ash contents compared to typical biomass test materials, the effects of these components to the thermal processing need to be considered. The slow pyrolysis system creates an environment that can promote the secondary reactions for the pyrolysis products produced in the primary thermal decomposition. For those runs under the high processing temperatures (over 600 °C), water are likely become a reagent in some reactions, and ash (a mixture of silicon and metal oxides) may become a catalyst. Hence, the mass balance of the thermal processing is presented on both dry and wet feed bases to examine the effects of different processing conditions over the product yield and distribution.

All three products (liquid, solid and gaseous) were collected and analysed. The liquids obtained were directly separated by gravity into organic and aqueous fractions (see Fig. S2 in Supplementary Material). All the organic fraction products had a lower density than the aqueous products and hence appeared in an upper layer. Fig. 3a–d presents the process mass balance of all analysed products on wet feed basis, and Fig. 3e presents the yields of organic and solid products of the pyrolysis reactions on dry feed basis. The yields of gaseous product cannot be presented on dry feed basis (particularly of those runs at 700 and 850 °C), as they were produced in both pyrolysis and secondary reactions, in which water was consumed (details discussed in the following sections). Both the dry and wet bases show the yields of char decrease with the temperature increase regardless the moisture content of the feedstock, but those of the organic liquid initially increased with the rise in processing temperature, reaching a peak at 550 °C for moisture contents of 45.8% and 34.6%, and 700 °C for 22.8% and 12.7% moisture contents. From Fig. 3a–d, it can be seen that, although the OFMSW feedstocks contained considerably different amounts of moisture, all of the product yields show a similar trend under the same processing temperature. Taking Fig. 3a (45.8% moisture content) as an example, the yields of both aqueous liquid product and char reduce when the processing temperature was increased from 450 to 850 °C, while those of gas increased noticeably (over 20%) at the same time. This is because the higher processing temperatures promote secondary reactions involving strong thermal cracking and reforming, resulting in an increase in permanent gas yield [28].

It is well known that, during pyrolysis, an increase in reaction temperature first leads to a drying stage (evaporation of moisture); then above about 150 °C, primary decomposition occurs, in which the heat triggers the thermal scission of chemical bonds in the individual constituents of raw material, resulting in progressive release of volatiles [29]. When processed at higher temperatures (over 600 °C) with a prolonged vapour residence time as in slow pyrolysis, the volatiles released in the primary reactions can interact with steam and hot char product in a variety of secondary reactions including cracking, reforming, and dehydration to produce lower molecular weight organics and gases [30]. Regression analysis confirmed there was a relatively strong relationship between gas yield and OFMSW processing temperature ($R^2 = 0.846$, $n = 16$, $p = 0.000$), compared to that between gas yield and OFMSW moisture content ($R^2 = 0.058$, $p = 0.003$).

As the moisture content of the feedstock reduces, the yields of aqueous liquid reduce accordingly, as less water is available to form the aqueous product. At the same time, the solid product becomes the highest yielding product when the feedstock moisture content is relatively low. This is due to the high ash content in the feedstock. When the moisture content is lower, the ash content is proportionally higher as yields are reported on a wet feed basis. All the ash remains in the solid product, consequently resulting in an increased solid yield.

All of the mass balances closures were above 90% (calculated mass losses less than 10%, as shown by black curves in Fig. 3). The losses in mass balance were due to some uncollectible heavy organic fractions of the liquid remaining on the liquid condensation tubes, as well as measurement errors and minor gas leaks during the experimental runs.

3.3. Product analysis

3.3.1. Liquid product

The appearance (colour and form) of the liquid products was noticeably different at different processing temperatures, with the aqueous fraction appearing less turbid and lighter in colour with increasing temperature. The liquid products collected from pyrolysis at 45.8% moisture content and varying processing temperatures are shown in Fig. S2.

The results of elemental analysis of the liquid and solid products are given in Table S3. For the organic fraction liquid, the carbon and hydrogen content decreased with an increase in processing temperature. This is due to the higher conversion of organic matter into permanent gases. The low carbon and hydrogen content results in low heating values for the organic liquid. For the aqueous fraction, carbon content decreased with increasing processing temperature, but the hydrogen content remains almost the same. This is simply because water is the major component, and hence the hydrogen and oxygen contents remain relatively stable. It is worth noting that the pH values of the aqueous fraction liquid products increase with rises in processing temperature (Fig. S3). At the same processing temperature, the high moisture content feedstock produced liquid with relatively higher pH values. This implies that the production of acidic chemicals is promoted when processing high moisture feedstock at low temperatures, while that of basic chemicals is promoted when processing low moisture feedstock at high temperatures. Further investigation of the chemical composition of the aqueous fraction products using GC–MS analysis (taking 45.8% moisture content feedstock as an example) showed that at a processing temperature of 450 °C, fluoroacetic acid and alcohols are the main organic compounds in the aqueous liquid; while at 850 °C, the main compounds are amines and pyrrole (see Fig. S4 and Table S4). As discussed in Section 3.2, the high processing temperature in slow pyrolysis promotes secondary reactions. The change in chemical composition in the aqueous products may be due to the promotion of basic chemicals in reforming and dehydration reactions.

3.3.2. Gas analysis

Fig. 4 presents the gas analysis results for the pyrolysis runs. The concentrations of major pyrolysis gas components including H_2, CO and CH_4 were measured. The residual components are primarily CO_2 with trace amounts of other gases (OG) consisting of gaseous hydrocarbon compounds (CmHn) such as ethane, ethylene, propane etc. Processing of feedstocks with high moisture and high ash contents at high temperature in the auger reactor creates a pyrolysis/gasification environment that promotes secondary reactions. The gas composition of the process is the combined result of a series of complex and competing secondary reactions, including the Boudouard reaction, water-gas shift reaction, methanation and steam reforming reactions [31,32]. There is also the possibility that these reactions are promoted by minor catalytic effects as a result of the presence of various metals (e.g. cobalt, nickel and iron) in the feedstock.

Comparison between Fig. 4a-d shows that the yields of different gas components are heavily influenced by processing temperature. At the same processing temperature, however, the feedstock moisture content did not noticeably affect the yield. Taking Fig. 4a as an example, H_2

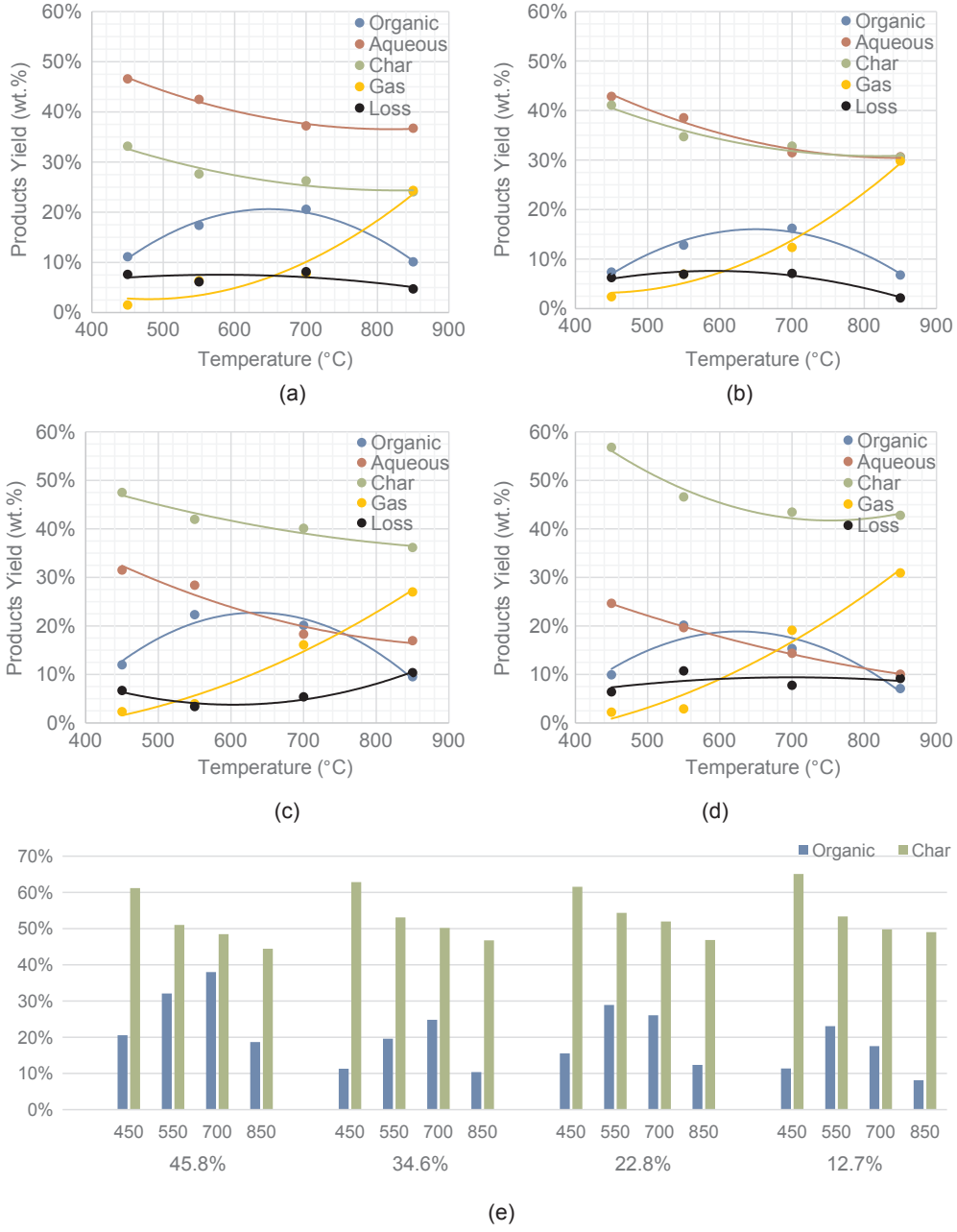

Fig. 3. Mass balances of the pyrolysis experiments under matrix conditions. (a) (b) (c) (d) presents the mass balance on web feed basis and their moisture contents are 45.8%, 34.6%, 22.8% and 12.7%, respectively; (e) presents the yields of organic and solid products on dry feed basis).

yields increased from less than 2% at 450 °C to over 40% at 850 °C, while yields of CO_2 and other gases were reduced from nearly 80% at 450 °C to 34% at 850 °C. A similar tendency is observed for all four moisture contents tested. Regression analysis confirmed this, with processing temperature accounting for around 89, 89 and 83% of the variation in H_2, CH_4 and CO_2 (with other gases) respectively, while moisture content had little effect on gas composition and neither parameter significantly influences CO content.

3.3.3. Char analysis

The results of elemental analysis of the char products are shown in Table S3. It can be seen that the processing temperature considerably affected the carbon and hydrogen contents of the char samples: regression analysis indicated that around 68% of the variation in C and 74% of the variation in H was accounted for by OFMSW processing temperature. An increase in processing temperature causes more removal of volatile organics from the feedstock to form pyrolysis vapour. Since ash and inert material in the feedstock are present in fixed amounts and always remain as a part of the solid product, the high processing temperature resulted in a high ash-content char. For all char samples, the ash content increased from 50 to 60% at 450 °C to about 85% at 850 °C and showed a relatively strong relationship with processing temperature (R^2 = 0.848, n = 16, p = 0.000). Some research has indicated that high moisture content could increase the char yield from typical biomass feedstocks [33]. However, it was found that the effect of feedstock moisture content on the char from OFMSW feedstock was relatively insignificant (R^2 = 0.018, p = 0.000).

3.3.4. Product energy distribution

Table 2 shows the calculated energy content of each fraction based on its elemental composition, and the energy partitioning between the fractions. Processing temperature had a strong effect on the product energy distribution, while the effect of feedstock moisture was relatively small. At 450 °C, the char product contained the highest energy (around 50–60% of the total for all products), followed by the organic fraction of the liquid product. When the processing temperature

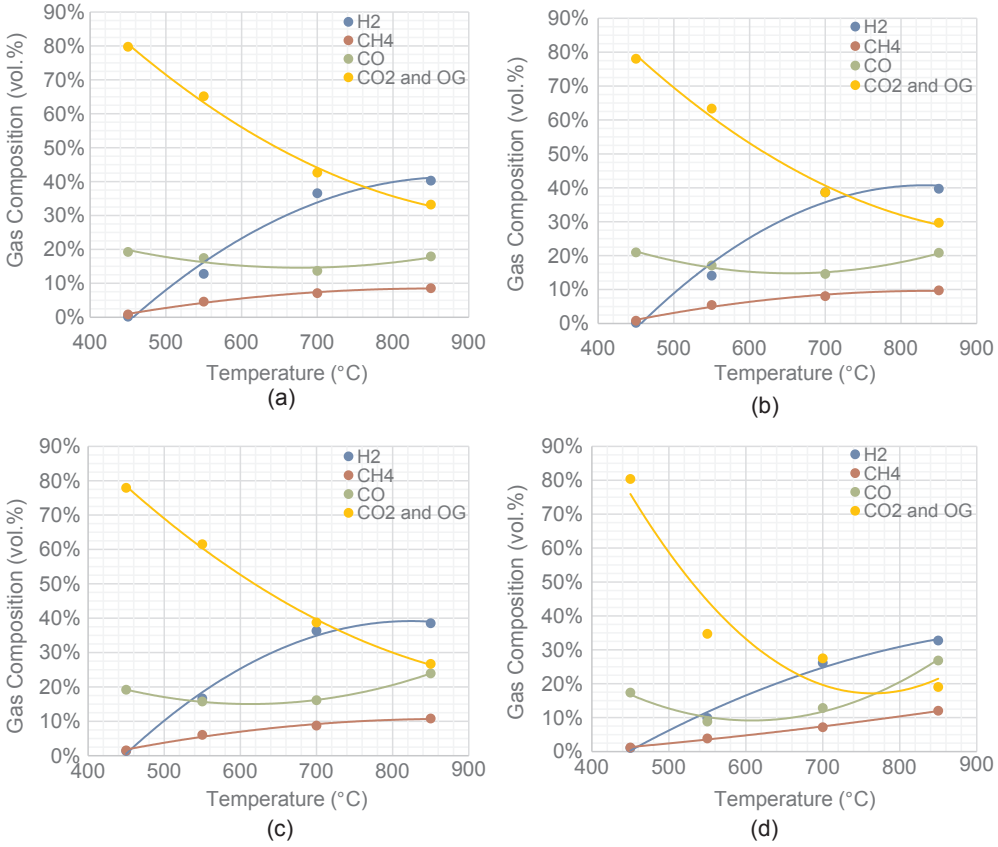

Fig. 4. Gas analysis of the pyrolysis experiments. Feedstock moisture content: (a) 45.8%; (b) 34.6%; (c) 22.8%; (d) 12.7%.

increases to 550 °C, the energy in the organic fraction exceeds that in the char, making the organic fraction the most energy abundant product. As the temperature increases further to 700 °C (close to the general gasification temperature), the pyrolysis gas contains the highest proportion of the energy, as a result of the high yield of gas containing an increased proportion of the combustible fraction (H_2 and CO). At 850 °C, over 60% of the product energy is in the gaseous product. The aqueous fraction of the liquid product contains the lowest proportion of

Table 2
Energy distribution in OFMSW production fractions.

Moisture	wt%	**45.8%**	**45.8%**	**45.8%**	**45.8%**	**34.6%**	**34.6%**	**34.6%**	**34.6%**	**22.8%**	**22.8%**	**22.8%**	**22.8%**	**12.7%**	**12.7%**	**12.7%**	**12.7%**
Temp	°C	**450**	**550**	**700**	**850**	**450**	**550**	**700**	**850**	**450**	**550**	**700**	**850**	**450**	**550**	**700**	**850**
Measured HHV																	
Organic	MJ/kg product	26.38	29.40	8.71	9.93	28.55	31.10	7.90	8.66	33.71	31.06	7.71	7.55	33.66	26.18	8.42	7.70
Aqueous	MJ/kg product	n/a	n/a	n/a	n/a	n/a	n/a	n/a	n/a	n/a	n/a	n/a	n/a	n/a	n/a	n/a	n/a
Char	MJ/kg product	10.20	6.60	5.10	3.70	11.60	7.90	4.80	3.70	9.20	5.40	5.90	4.50	10.80	6.20	5.80	4.70
Gas	MJ/kg product	n/a	n/a	n/a	n/a	n/a	n/a	n/a	n/a	n/a	n/a	n/a	n/a	n/a	n/a	n/a	n/a
Calculated HHV[a]																	
Organic	MJ/kg product	24.92	29.87	7.78	9.52	32.14	30.17	3.38	14.19	29.90	30.65	7.67	3.86	36.26	27.11	10.44	12.16
Aqueous	MJ/kg product	2.23	1.59	1.12	0.54	2.08	1.85	1.20	0.69	2.71	2.63	1.71	0.91	3.73	3.20	2.24	1.16
Char	MJ/kg product	11.62	6.92	5.26	4.17	11.95	6.98	5.96	4.68	10.64	7.63	5.90	5.89	12.33	7.83	8.51	6.95
Gas	MJ/kg product	2.94	3.67	8.44	11.09	3.08	4.06	9.65	12.20	3.11	4.46	9.60	13.08	2.93	4.75	10.05	14.90
Energy content[b]																	
Organic	MJ/kg OFMSW	2.77	5.20	1.60	0.96	2.37	3.87	0.75	0.96	3.58	6.84	1.54	0.37	3.60	5.46	1.60	0.86
Aqueous	MJ/kg OFMSW	1.04	0.68	0.42	0.20	0.89	0.71	0.38	0.21	0.86	0.75	0.31	0.15	0.92	0.63	0.32	0.12
Char	MJ/kg OFMSW	3.85	1.91	1.07	1.00	4.91	2.42	1.54	1.43	5.06	3.20	1.90	2.13	7.00	3.65	2.85	2.97
Gas	MJ/kg OFMSW	0.27	0.46	1.85	3.22	0.27	0.56	1.97	3.90	0.28	0.33	2.83	4.89	0.25	0.65	3.70	5.97
Total	MJ/kg OFMSW	7.94	8.24	4.93	5.39	8.44	7.57	4.64	6.51	9.77	11.12	6.58	7.54	11.77	10.38	8.47	9.93
%[b]		51.5	53.5	32.0	35.0	54.8	49.1	30.1	42.2	63.5	72.2	42.7	48.9	76.4	67.4	55.0	64.5
Energy proportion[c]																	
Organic	%	35.0	63.0	32.5	17.9	28.1	51.1	16.2	14.8	36.7	61.5	23.4	4.9	30.6	52.6	18.9	8.7
Aqueous	%	13.1	8.2	8.5	3.7	10.5	9.4	8.1	3.2	8.7	6.7	4.8	2.0	7.8	6.0	3.8	1.2
Char	%	48.6	23.2	21.6	18.6	58.2	32.0	33.2	22.0	51.7	28.8	28.8	28.2	59.5	35.1	33.6	30.0
Gas	%	3.3	5.6	37.4	59.8	3.2	7.5	42.5	60.0	2.9	3.0	43	64.9	2.1	6.3	43.7	60.1

n/a = not available.

[a] HHV calculated from elemental composition using Dulong equation [24].

[b] Sum of energy in individual product fractions expressed as a percentage of the measured HHV of the original OFMSW.

[c] Energy in individual product fractions expressed as a percentage of the energy content of all fractions.

the energy in all cases, accounting for about 10–13% at low processing temperatures decreasing to 1–4% at higher processing temperatures.

Regression analysis indicated that processing temperature alone accounted for about 94% of the variation in HHV and 84% of the variation in energy content of the gaseous product, rising to 96% and 90% respectively if the moisture content of the OFMSW sample is also taken into account. For the aqueous fraction the equivalent values were around 65 and 95% of HHV and energy content respectively for processing temperature alone, rising to 92% and 96% respectively if the OFMSW moisture content is taken into account. Regression coefficients for the relationships between OFMSW processing temperature and moisture content with the energy content of other fractions and the total energy recovered in all fractions were generally lower, but these results indicate the potential for predicting with some confidence the energy partitioning into at least two of the produced fractions.

Results of regression analysis and predictive equations for properties of pyrolysis products are given in Table S5.

3.4. AD trials on aqueous liquid product

3.4.1. COD parameters

COD was measured as part of the anaerobic biodegradability screening, as this unit is commonly used in reporting organic loading rates and can be converted stoichiometrically to give a potential methane yield.

Fig. 5 shows the COD content of the aqueous fractions. Both the moisture content of the OFMSW and the processing temperature affected the COD concentration. An increase in processing temperature from 450 to 550 °C had relatively little effect on the COD for samples at all moisture contents; but as the processing temperature increased further, the COD concentration fell and the difference between samples at different initial moisture contents reduced (Fig. 5a). This reduction in COD with increasing temperature reflects the fall in carbon content noted above.

The COD of the aqueous fraction was inversely proportional to moisture content at all processing temperatures (Fig. 5b), with the COD concentration at 450 °C about twice that at 850 °C. At 850 °C the difference in absolute values was relatively small, but increased considerably at the lower processing temperatures. The COD concentrations at 450 and 550 °C were fairly similar at all moisture contents.

Regression analysis showed that the relationship between COD and processing temperature was relatively strong ($R^2 = 0.702$, $p = 0.000$, $n = 32$), while that between COD and OFMSW moisture content was weaker ($R^2 = 0.189$, $p = 0.0130$). When both factors are combined, however, a predictive equation for COD content of the aqueous fraction can be obtained with a combined coefficient of $R^2 = 0.89$ (Fig. 5c), implying that these two parameters explain almost 90% of the variation in COD. The relationships between OFMSW properties and COD content of the aqueous fraction thus reflected those found above for aqueous fraction.

The COD yield in the aqueous fraction can be calculated from the COD concentration of the aqueous fraction and the moisture content of the OFMSW sample. The results are shown in Fig. 5d. At processing temperatures of 450 and 550 °C the average COD yield was around 56 g COD kg^{-1} dry weight of OFMSW for moisture contents of 45.8, 34.6 and 22.8%, and was only slightly lower at around 33 g COD kg^{-1} OFMSW for moisture content 12.7%. If this COD can be converted into methane, it represents around 0.8 MJ kg^{-1} OFMSW, or 5% of the measured HHV of the OFMSW. At 850 °C and 12.7% moisture content, the COD yield is one tenth of that at lower process temperatures and

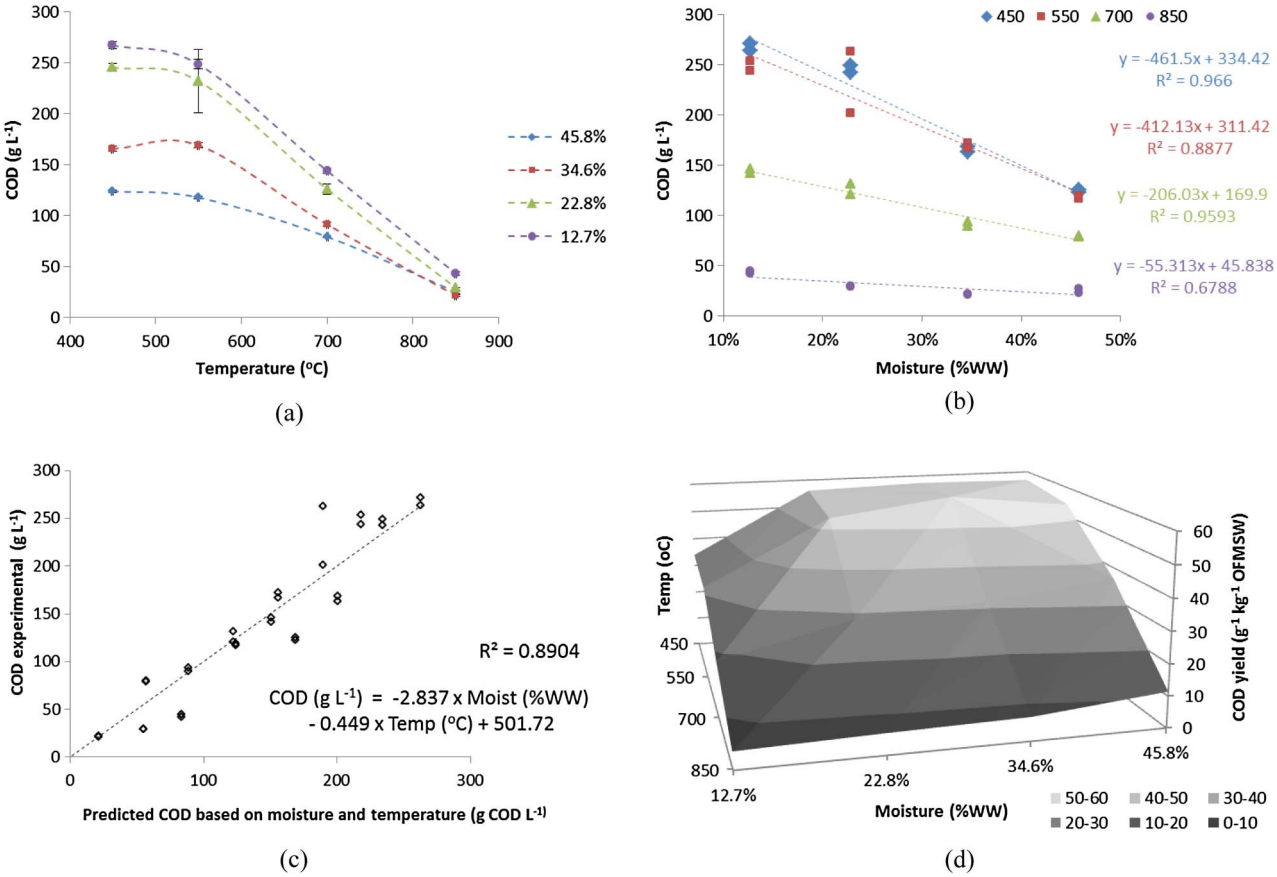

Fig. 5. COD parameters for the aqueous fraction pyrolysis products. (a) Variation of COD with processing temperature at a given moisture content; (b) variation of COD with moisture content at a given processing temperature; (c) predictive equation for aqueous fraction COD content based on moisture content and processing temperature; (d) COD yield in the aqueous fraction per unit wet weight of OFMSW.

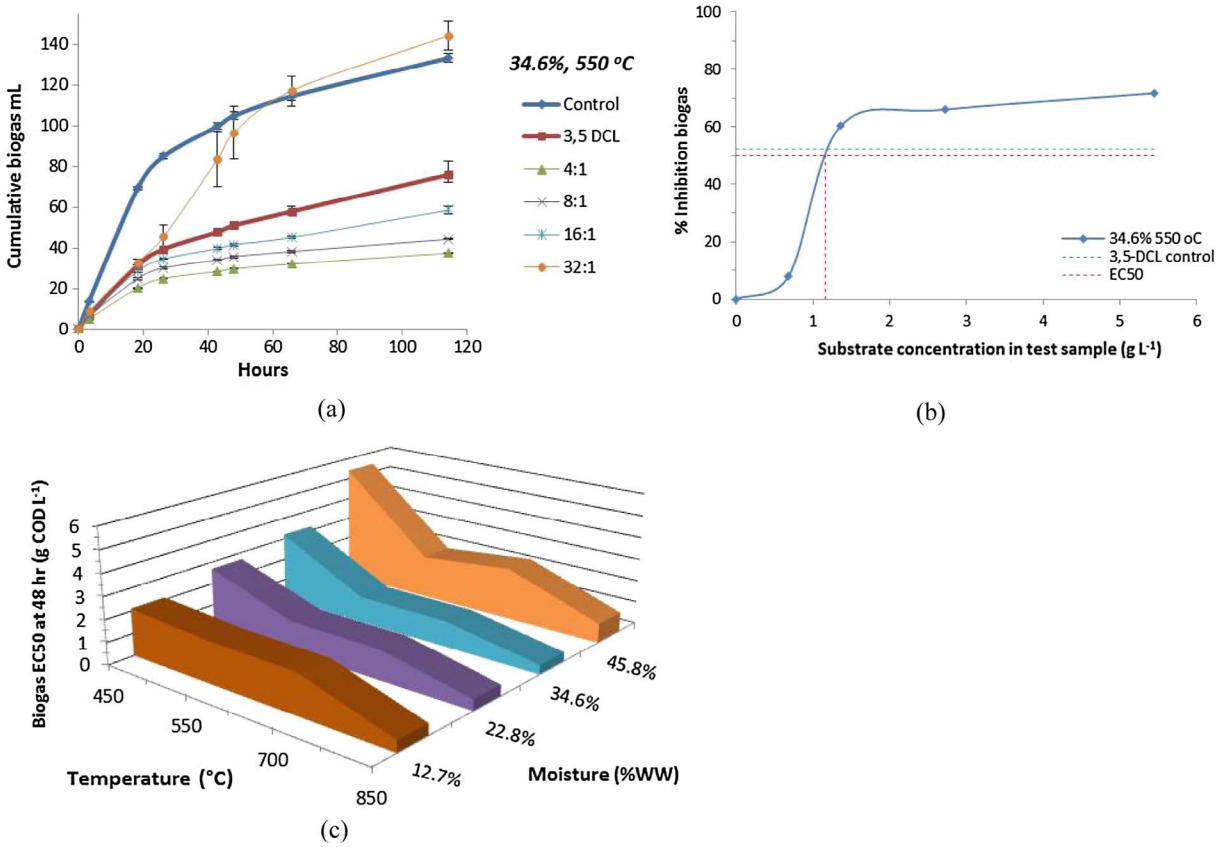

Fig. 6. Results of anaerobic toxicity testing of aqueous fraction. (a) cumulative biogas production and (b) EC50 determination for 34.6% moisture, 550 °C; (c) EC50.

higher moisture contents. For anaerobic digestion to be worthwhile a reasonable methane yield must be achievable, and the type of process and reactor used will depend on the COD concentration and flow rate; but the main factor determining feasibility will be the energy balance of the overall process including all pyrolysis components.

3.4.2. Toxicity assay

Fig. 6a shows typical results for a toxicity assay, in this case for the 34.6% moisture content sample treated at 550 °C, in which the cumulative biogas production values are well distributed with respect to the controls and in general show good replication. There is some variation between the replicates at i/s ratio 32:1 after 48 h. This is probably due both to the higher dilution, and to the fact that these samples initially showed inhibition during the first 60 h of the test, before recovering to give a positive net biogas yield: behaviour during onset of and recovery from inhibition often shows variable responses of this type. Fig. 6b shows the processed results for this sample, from which the EC50 value is obtained. The calculated value of EC50 shows good agreement with the 3,5-DCL positive control in this case. In other cases, there was some variation in the values for the positive control, but the EC50 value was always based on the average result for the inoculum only controls. Results for all conditions tested are given in Fig. S5.

Fig. 6c shows the EC50 values taken at 48 h from the start of the test for the whole matrix of conditions, expressed in terms of g COD L^{-1} of sample added. In general, the toxicity of the aqueous fraction increases with increasing process temperature and decreasing moisture content of the OFMSW sample: the aqueous fraction of the OFMSW sample processed at 12.7% moisture and 850 °C causes 50% inhibition at a test assay concentration of around 0.5 g COD L^{-1}, less than one tenth of the value of 5.4 g COD L^{-1} for the sample processed at 45.8% moisture and 450 °C. Correlation coefficients between EC50 and OFMSW moisture content, processing temperature and the COD content of the original undiluted aqueous fraction sample were $R^2 = 0.09$, 0.54 and 0.15 respectively (n = 16), indicating that processing temperature was the dominant factor affecting toxicity. Combining the independent parameters of moisture and processing temperature accounted for 80% of the variation in EC50.

Fig. 7a shows the full set of results for cumulative net specific methane production (cnSMP) at the end of the test runs. The results here are grouped by dilution and moisture content: an alternative presentation is given in the Supplementary materials. Although some individual results are erratic, a number of trends can be clearly seen. In general, cnSMP decreases with increasing OFMSW processing temperature, in line with the increase in toxicity seen in the EC50 results. At 850 °C most cnSMP values are strongly negative, and decrease with increasing i/s ratio. This is explained by the fact that biogas production is strongly inhibited in these cases. At 12.7% moisture and 850 °C, for example, the average cumulative biogas production was 4.7, 14.7, 25.1 and 47.1 mL at i/s ratios of 4:1. 8:1, 16:1 and 32:1 respectively, well below the 123.9 mL produced by the inoculum-only controls. Net biogas and methane production was therefore negative in each case and, since the amount of COD added is inversely proportional to the dilution, the specific biogas and methane productions are progressively more negative with increasing i/s ratio.

At a given OFMSW moisture content, as the processing temperature decreases the amount of biogas and methane produced increases until positive values for cnSMP start to appear. At higher dilutions, the toxicity is further reduced and in general the cnSMP is higher, although there are some inconsistencies in measured values at the highest dilutions as a result of the small volumes of aqueous fraction added, the low volumes of gas produced and the effect of the high dilution factor in multiplying any measurement errors. At an i/s ratio of 4:1 the cnSMP was negative for the whole matrix of processing conditions tested. Positive cnSMP values for i/s 8:1, 16:1 and 32:1 occur only at 45.8% moisture and 450 °C. In these processing conditions, the cnSMP was 0.198 and 0.187 L CH_4 g^{-1} COD added for both of the higher dilutions

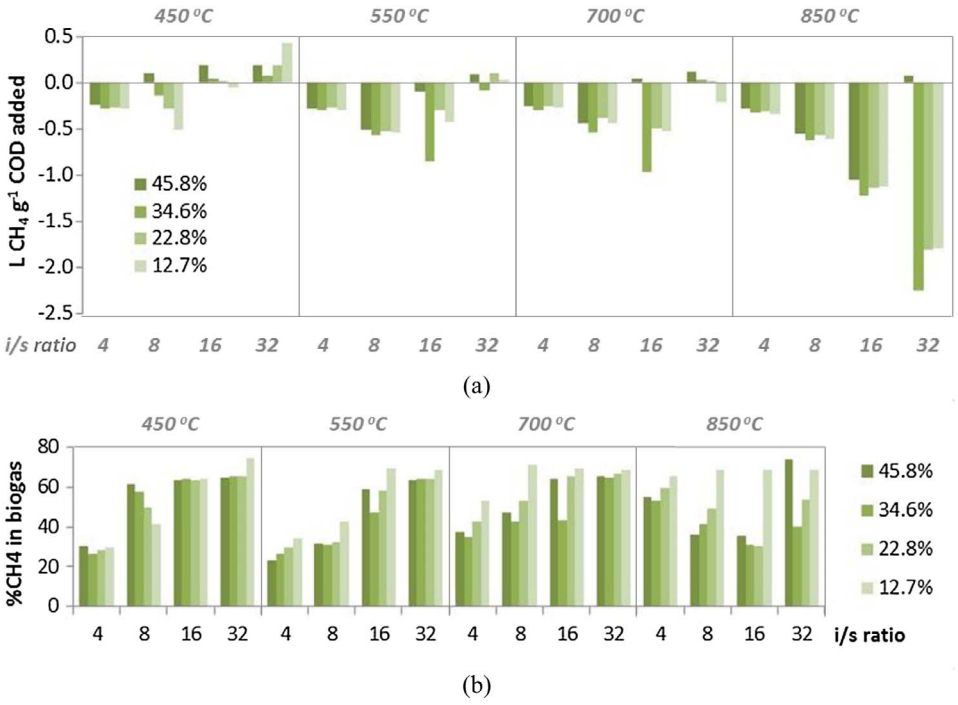

Fig. 7. Methane production during testing of aqueous fraction samples: (a) cnSMP and (b) biogas methane content for all samples against moisture and processing temperature.

(i/s 16:1 and 32:1). These values may be taken as an estimate of the specific methane potential of the aqueous fraction produced under these processing conditions. They represent about 57 and 53% respectively of the theoretical methane potential of the COD in the aqueous fraction, indicating that the remaining portion may be recalcitrant to anaerobic biodegradation. This is slightly higher than the 34% of theoretical methane yield achieved by Torri and Fabbri [16] for pyrolysis of cornstalk at 400 °C without addition of biochar. Coupled with the EC50 and cnSMP values, however, these results suggest for successful digestion of the aqueous fraction acclimatisation of the microbial consortium to the applied substrate and loading may be necessary, even under the most favourable OFMSW processing conditions.

The proportion of methane in the produced biogas at the end of the run is shown in Fig. 7b: this was affected by the OFMSW processing conditions, and also by the degree of dilution of the aqueous fraction sample. At processing temperatures up to 700 °C and moisture contents from 22.8 to 45.8%, the biogas methane content at the highest i/s ratio appeared to stabilise at around 64–65%. The methane content at 450 °C was also around 64% at i/s ratio 16:1, confirming that these conditions were not severely inhibited and may accurately represent the substrate methane potential. The method used is evidently able in principle to allow assessment of both EC50 and BMP values, although the toxicity of the materials tested in this case meant that only the most dilute samples showed positive net gas production, limiting the accuracy of the final BMP value.

Correlation coefficients between cnSMP and OFMSW moisture content, OFMSW processing temperature and the COD concentration of the original aqueous fraction sample at an i/s ratio of 16:1 were $R^2 = 0.02$, 0.70 and 0.40 respectively (n = 16). Biogas methane content at an i/s ratio of 8:1 showed a slightly stronger correlation with all three parameters with $R^2 = 0.07$, 0.81 and 0.49 for moisture content, processing temperature and COD concentration respectively, indicating once again that processing temperature is a key factor affecting degradability and methane yield: this also agrees with the findings of Hubner and Mumme [15]. Combining the effects of moisture and processing temperature in a single equation increased the R^2 value to 0.88.

3.5. Implications of the results of product characterisation

For pyrolysis, as expected, the processing temperature and, to a lesser extent, the feed moisture content affected the quantity and properties of the various pyrolysis product fractions. The relationships obtained in this work showed that the product mix and the overall energy yield can be predicted with reasonable accuracy, providing a basis for selection of the optimum process conditions for different end products and purposes. However, it is important to note that the energy requirement for drying the OFMSW to the relevant moisture contents was not taken into account in considering the energy yield.

For AD, the aqueous fraction has a relatively high COD content, in principle making it an attractive substrate for energy recovery through anaerobic digestion; and making treatment as a main or co-substrate in conventional stirred tank reactors feasible as well as in high-rate systems. In practice, however, the low EC50 values and the fact that toxicity varied considerably with the OFMSW moisture content and processing temperature may reduce the range of processing conditions that can usefully be applied. The low proportion of energy present in this fraction, and the fact that not all of this is accessible to anaerobic degradation, may also mean that anaerobic treatment is economically unattractive in many cases. To better understand the proportion of energy that can be recovered from the aqueous fraction, there is a need for continuous digestion studies where the effects of acclimatisation to the substrate can be determined.

4. Conclusions

- The liquid products from slow pyrolysis of OFMSW were clearly separated into an organic and an aqueous fraction by gravity.
- There were relatively strong effects of the processing temperature over the product yields and their energy contents, but the effects of feedstock moisture content on those were low. To maximise the organic liquid yield and minimise the process energy consumption in pyrolysis stage, low moisture content feedstock should be processed.
- The production of acidic chemicals is promoted when processing high moisture feedstock at low temperatures, while that of basic chemicals is promoted when processing low moisture feedstock at

high temperatures. The aqueous fraction changed from acidic to basic as processing temperatures increased.

- The pyrolysis processing temperature was the dominant factor affecting toxicity and COD of the aqueous liquid products. The higher the processing temperate, the higher the toxicity but the lower the COD content.
- The aqueous liquid contained 1.2–13.1% of the energy in the original OFMSW feedstock, but theoretically only around 50% was convertible to methane.
- In real waste management applications, anaerobic digestion of aqueous liquids from slow pyrolysis of OFMSW can be a method to increase the total energy recovery from waste, but probably by not more than 6.6%. The overall efficiency improvement may be insufficient to balance the additional cost of biological processing.

Acknowledgements

The financial support of this work was provided by the UK's Engineering and Physical Sciences Research Council (EPSRC) under the project reference number EP/K036793/1, SUPERGEN PyroAD. The authors are grateful to Dr Junmeng Cai of Shanghai Jiao Tong University for his significant contribution to the pyrolysis experiments.

Appendix A. Supplementary material

Supplementary data associated with this article can be found, in the online version, at http://dx.doi.org/10.1016/j.apenergy.2018.01.018.

References

[1] Eurostat. Municipal waste statistics; 2017. http://ec.europa.eu/eurostat/statistics-explained/index.php/Municipal_waste_statistics#Municipal_waste_treated_in_Europe [accessed September 1, 2017].
[2] Grosso M, Motta A, Rigamonti L. Efficiency of energy recovery from waste incineration, in the light of the new Waste Framework Directive. Waste Manag 2010;30:1238–43. http://dx.doi.org/10.1016/j.wasman.2010.02.036.
[3] Burnley S, Phillips R, Coleman T, Rampling T. Energy implications of the thermal recovery of biodegradable municipal waste materials in the United Kingdom. Waste Manag 2011;31:1949–59. http://dx.doi.org/10.1016/j.wasman.2011.04.015.
[4] Yang Y, Brammer JG, Wright DG, Scott JA, Serrano C, Bridgwater AV. Combined heat and power from the intermediate pyrolysis of biomass materials: performance, economics and environmental impact. Appl Energy 2017;191:639–52. http://dx.doi.org/10.1016/j.apenergy.2017.02.004.
[5] Chen D, Yin L, Wang H, He P. Pyrolysis technologies for municipal solid waste: A review. Waste Manag 2014;34:2466–86. http://dx.doi.org/10.1016/j.wasman.2014.08.004.
[6] Yang Y, Brammer JG, Ouadi M, Samanya J, Hornung A, Xu HM, et al. Characterisation of waste derived intermediate pyrolysis oils for use as diesel engine fuels. Fuel 2013;103:247–57. http://dx.doi.org/10.1016/j.fuel.2012.07.014.
[7] Czernik S, Bridgwater AV. Overview of applications of biomass fast pyrolysis oil. Energy Fuels 2004;18:590–8. http://dx.doi.org/10.1021/ef034067u.
[8] Yang Y, Brammer JG, Mahmood ASN, Hornung A. Intermediate pyrolysis of biomass energy pellets for producing sustainable liquid, gaseous and solid fuels. Bioresour Technol 2014;169:794–9. http://dx.doi.org/10.1016/j.biortech.2014.07.044.
[9] Mata-Alvarez J, Macé S, Llabrés P. Anaerobic digestion of organic solid wastes. An overview of research achievements and perspective. Bioresour Technol 2000;74:3–16. http://dx.doi.org/10.1016/S0960-8524(00)00023-7.
[10] Ariunbaatar J, Panico A, Esposito G, Pirozzi F, Lens PNL. Pretreatment methods to enhance anaerobic digestion of organic solid waste. Appl Energy 2014;123:143–56. http://dx.doi.org/10.1016/j.apenergy.2014.02.035.
[11] Fabbri D, Torri C. Linking pyrolysis and anaerobic digestion (Py-AD) for the conversion of lignocellulosic biomass. Curr Opin Biotechnol 2016;38:167–73. http://dx.doi.org/10.1016/j.copbio.2016.02.004.
[12] Salman CA, Schwede S, Thorin E, Yan J. Enhancing biomethane production by integrating pyrolysis and anaerobic digestion processes. Appl Energy 2017;204:1074–83. http://dx.doi.org/10.1016/j.apenergy.2017.05.006.
[13] Corton J, Donnison IS, Patel M, Bühle L, Hodgson E, Wachendorf M, et al. Expanding the biomass resource: sustainable oil production via fast pyrolysis of low input high diversity biomass and the potential integration of thermochemical and biological conversion routes. Appl Energy 2016;177:852–62. http://dx.doi.org/10.1016/j.apenergy.2016.05.088.
[14] Elsamadony M, Tawfik a, Suzuki M. Surfactant-enhanced biohydrogen production from organic fraction of municipal solid waste (OFMSW) via dry anaerobic digestion. Appl Energy 2015;149:272–82. http://dx.doi.org/10.1016/j.apenergy.2015.03.127.
[15] Hubner T, Mumme J. Integration of pyrolysis and anaerobic digestion – use of aqueous liquor from digestate pyrolysis for biogas production. Bioresour Technol 2015;183:86–92. http://dx.doi.org/10.1016/j.biortech.2015.02.037.
[16] Torri C, Fabbri D. Biochar enables anaerobic digestion of aqueous phase from intermediate pyrolysis of biomass. Bioresour Technol 2014;172:335–41. http://dx.doi.org/10.1016/j.biortech.2014.09.021.
[17] Monlau F, Sambusiti C, Antoniou N, Zabaniotou A, Solhy A, Barakat A. Pyrochars from bioenergy residue as novel bio-adsorbents for lignocellulosic hydrolysate detoxification. Bioresour Technol 2015;187:379–86. http://dx.doi.org/10.1016/j.biortech.2015.03.137.
[18] Erdogan E, Atila B, Mumme J, Reza MT, Toptas A, Elibol M, et al. Characterization of products from hydrothermal carbonization of orange pomace including anaerobic digestibility of process liquor. Bioresour Technol 2015;196:35–42. http://dx.doi.org/10.1016/j.biortech.2015.06.115.
[19] Monlau F, Sambusiti C, Antoniou N, Barakat A, Zabaniotou A. A new concept for enhancing energy recovery from agricultural residues by coupling anaerobic digestion and pyrolysis process. Appl Energy 2015;148:32–8. http://dx.doi.org/10.1016/j.apenergy.2015.03.024.
[20] Monlau F, Francavilla M, Sambusiti C, Antoniou N, Solhy A, Libutti A, et al. Toward a functional integration of anaerobic digestion and pyrolysis for a sustainable resource management. Comparison between solid-digestate and its derived pyrochar as soil amendment. Appl Energy 2016;169:652–62. http://dx.doi.org/10.1016/j.apenergy.2016.02.084.
[21] Yu Y, Yang Y, Cheng Z, Blanco PH, Liu R, Bridgwater AV, et al. Pyrolysis of rice husk and corn stalk in auger reactor: Part 1. Characterization of char and gas at various temperatures. Energy Fuels 2016;30:10568–74. http://dx.doi.org/10.1021/acs.energyfuels.6b02276.
[22] APHA. Standard methods for the examination of water and wastewater. 21st ed. Washington, DC (USA); American Public Health Association, American Water Works Association, Water Environment Federation; 2005.
[23] SCA. The determination of chemical oxygen demand in waters and effluents. In: Methods for the examination of waters and associated materials, standing committee of analysts; 2007. https://www.gov.uk/government/uploads/system/uploads/attachment_data/file/316793/COD-215nov.pdf [accessed August 1, 2017].
[24] IFRF. File 24 in combustion handbook; 2017. http://www.handbook.ifrf.net/handbook/cf.html?id=24 [accessed October 1, 2017].
[25] Banks SW, Nowakowski DJ, Bridgwater AV. Impact of potassium and phosphorus in biomass on the properties of fast pyrolysis bio-oil. Energy and Fuels 2016;30:8009–18. http://dx.doi.org/10.1021/acs.energyfuels.6b01044.
[26] Cai J, Xu D, Dong Z, Yu X, Yang Y, Banks SW, et al. Processing thermogravimetric analysis data for isoconversional kinetic analysis of lignocellulosic biomass pyrolysis: case study of corn stalk. Renew Sustain Energy Rev 2018;82(Part 3):2705–15.
[27] Cai J, He Y, Yu X, Banks SW, Yang Y, Zhang X, et al. Review of physicochemical properties and analytical characterization of lignocellulosic biomass. Renew Sustain Energy Rev 2017;76:309–22. http://dx.doi.org/10.1016/j.rser.2017.03.072.
[28] Bridgwater AV. Review of fast pyrolysis of biomass and product upgrading. Biomass Bioenergy 2012;38:68–94. http://dx.doi.org/10.1016/j.biombioe.2011.01.048.
[29] Neves D, Thunman H, Matos A, Tarelho L, Gómez-Barea A. Characterization and prediction of biomass pyrolysis products. Prog Energy Combust Sci 2011;37:611–30. http://dx.doi.org/10.1016/j.pecs.2011.01.001.
[30] Yin C. Microwave-assisted pyrolysis of biomass for liquid biofuels production. Bioresour Technol 2012;120:273–84. http://dx.doi.org/10.1016/j.biortech.2012.06.016.
[31] Görling M, Larsson M, Alvfors P. Bio-methane via fast pyrolysis of biomass. Appl Energy 2013;112:440–7. http://dx.doi.org/10.1016/j.apenergy.2013.01.002.
[32] Wang N, Chen D, Arena U, He P. Hot char-catalytic reforming of volatiles from MSW pyrolysis. Appl Energy 2017;191:111–24. http://dx.doi.org/10.1016/j.apenergy.2017.01.051.
[33] Manyà JJ. Pyrolysis for biochar purposes: a review to establish current knowledge gaps and research needs. Environ Sci Technol 2012;46:7939–54. http://dx.doi.org/10.1021/es301029g.